

Supplementary Information

Influence of Zn on the Photoluminescence of Colloidal $(\text{AgIn})_x\text{Zn}_{2(1-x)}\text{S}_2$ Nanocrystals

Dharmendar Kumar Sharma, Shuzo Hirata, Lukasz Bujak, Vasudevanpillai Biju, Tatsuya Kameyama, Marino Kishi, Tsukasa Torimoto, Martin Vacha

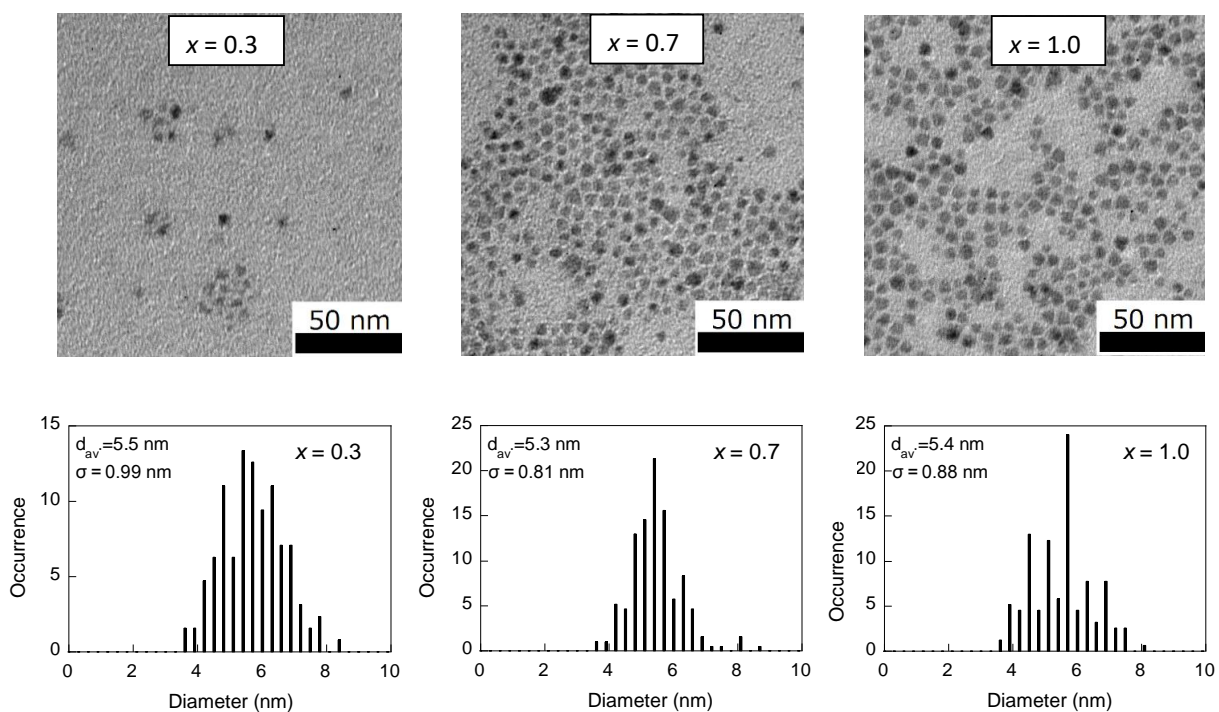


Figure S1. TEM images (top) and distributions of particle size (bottom) of the three compositions. The size distributions contain the statistical parameters of average size d_{av} and standard deviation σ .

x	Ag	In	Zn
0.3	14	22	64
0.7	34	40	26
1.0	48	52	0.0

Table S1. Elemental composition of the synthesized ZAIS nanocrystals measured by EDX

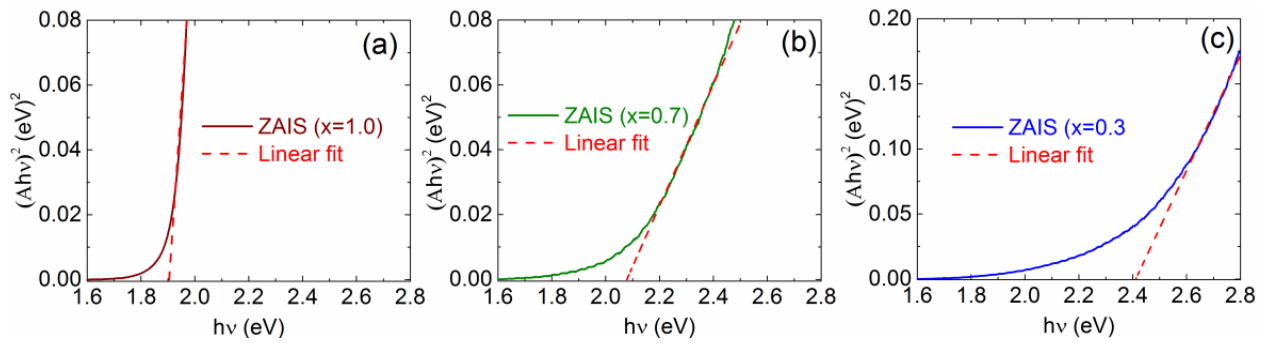


Figure S2. Estimation of E_g using linear part of $Ah\nu^2$ vs. $h\nu$ plot.

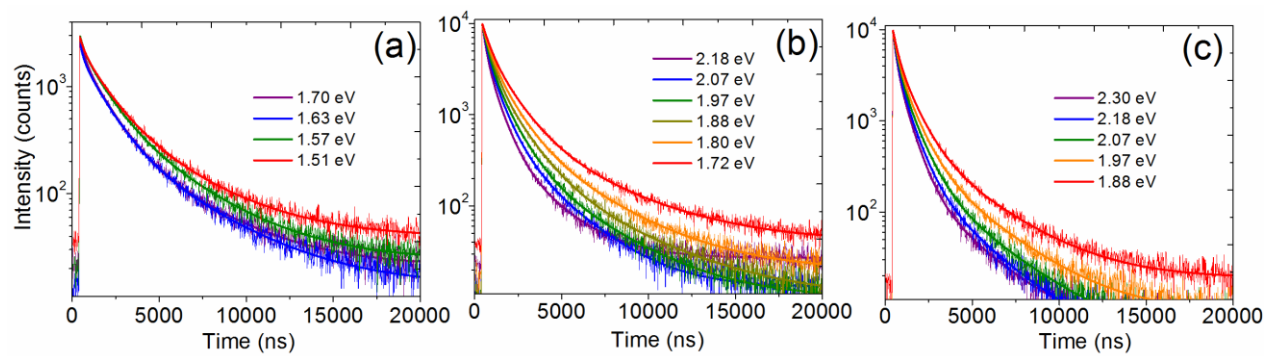


Figure S3 Three-exponential-fitted PL intensity decay curves of ZAIS $x = 0.3$ (a), $x = 0.7$ (b) and $x = 1.0$ (c) NCs at 3.4 eV excitation. The legends indicate the monitoring PL energy.

$E_{PL}(eV)$	$\langle\tau\rangle$ (ns)	τ_1	τ_2	τ_3	α_1	α_2	α_3
x=0.3							
2.30	811	177	620	2454	0.56	0.41	0.02
2.18	878	209	678	2450	0.56	0.41	0.03
2.07	1017	260	798	2909	0.57	0.39	0.03
1.97	1174	264	818	2899	0.51	0.44	0.05
1.88	1388	264	855	3071	0.44	0.49	0.07
x=0.7							
2.18	929	211	670	2243	0.52	0.43	0.05
2.07	1104	234	736	2496	0.47	0.46	0.06
1.97	1294	326	988	3345	0.56	0.40	0.04
1.88	1518	436	1298	4261	0.64	0.33	0.03
1.80	1647	414	1160	3639	0.50	0.43	0.06
1.72	1947	428	1272	4181	0.45	0.48	0.07
x=1.0							
1.70	2194	237	1213	3770	0.32	0.55	0.13
1.63	2353	183	1227	3967	0.28	0.58	0.14
1.57	2388	240	1261	3684	0.24	0.57	0.19
1.51	2518	265	1330	3814	0.22	0.57	0.21

Table S2. Energy dependent PL decay constants and their relative contributions. The averages of the decay times are calculated using $\langle\tau\rangle = \sum_i \frac{\alpha_i \tau_i^2}{\alpha_i \tau_i}$.

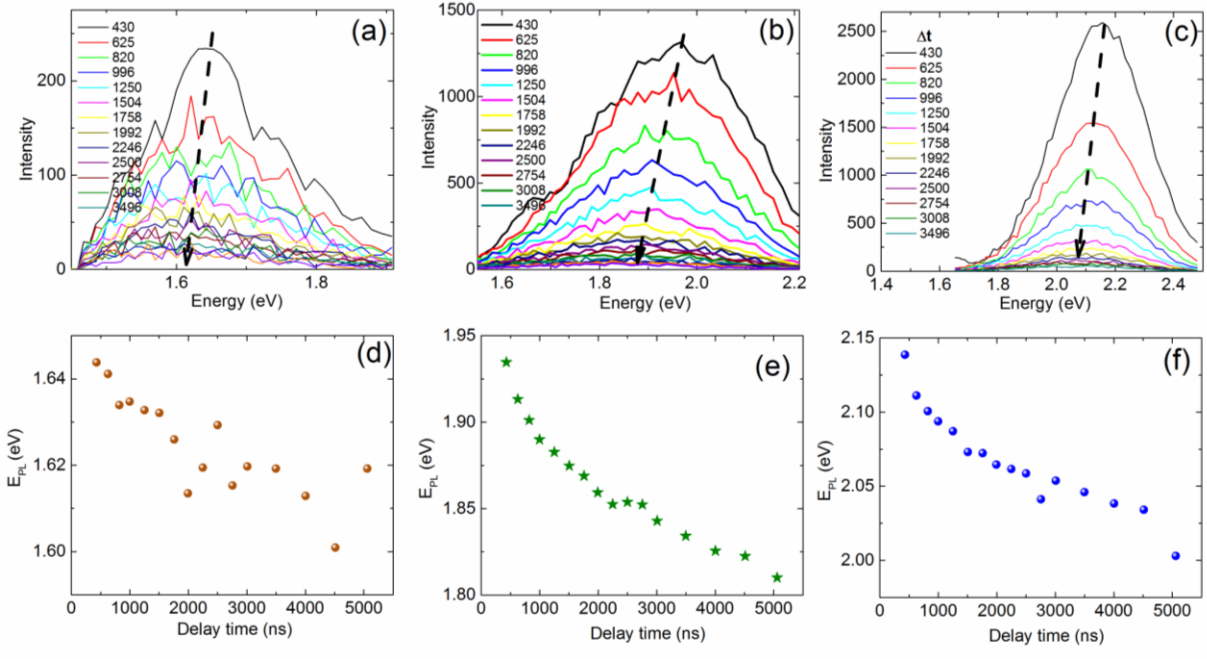


Figure S4 Time-resolved PL spectra of ZAIS NCs for $x=1.0$ (a), 0.7 (b) and 0.3 (c) at RT. The delay times used to reconstruct the spectra are shown in the legends in the units of ns. The peak energies of the time-resolved PL spectra were estimated by spectral fitting analysis assuming a Gaussian profile of PL and were plot for each composition ‘ x ’ in (d-f).

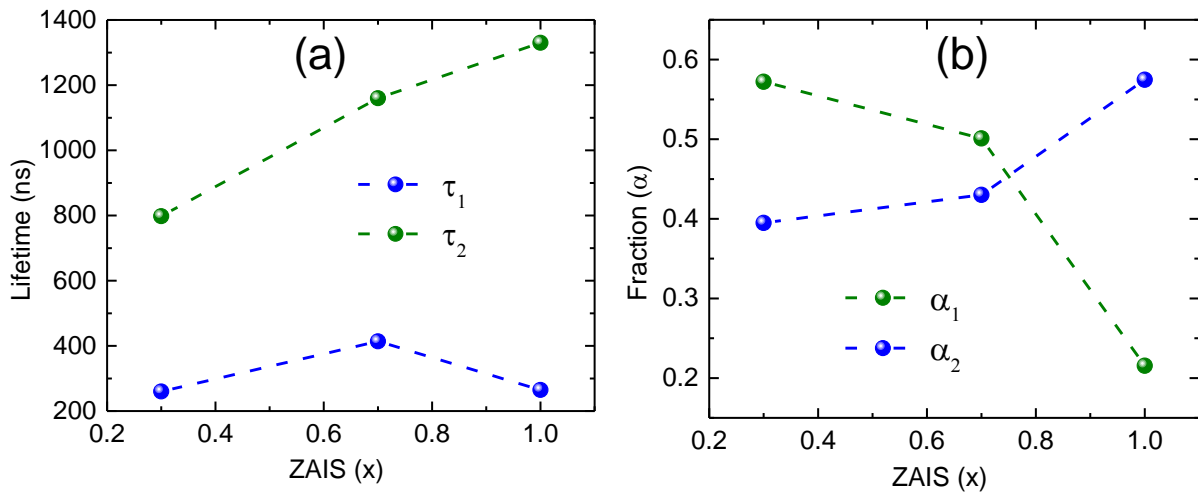


Figure S5 Complimentary dependence of lifetimes τ_1 and τ_2 (a), and their fractions α_1 and α_2 (b) with the increasing x (decreasing Zn) in ZAIS.

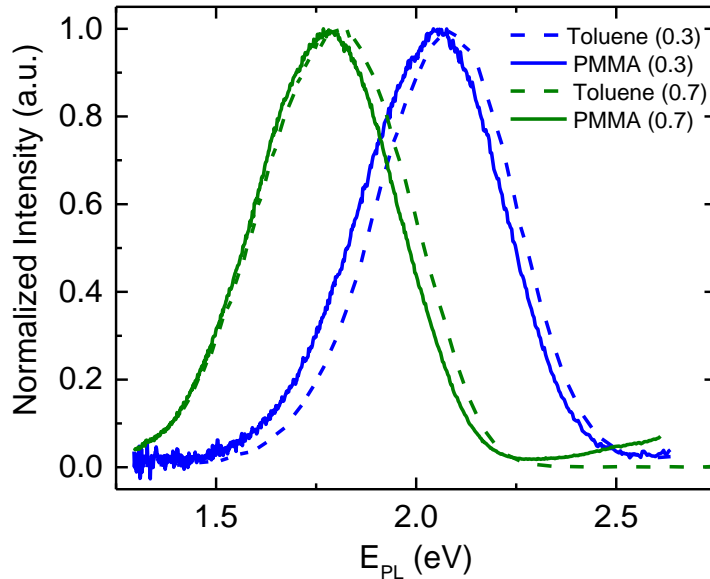


Figure S6 Normalized PL spectra of ZAIS ($x=0.3$, blue and 0.7 , green) in toluene and PMMA film.

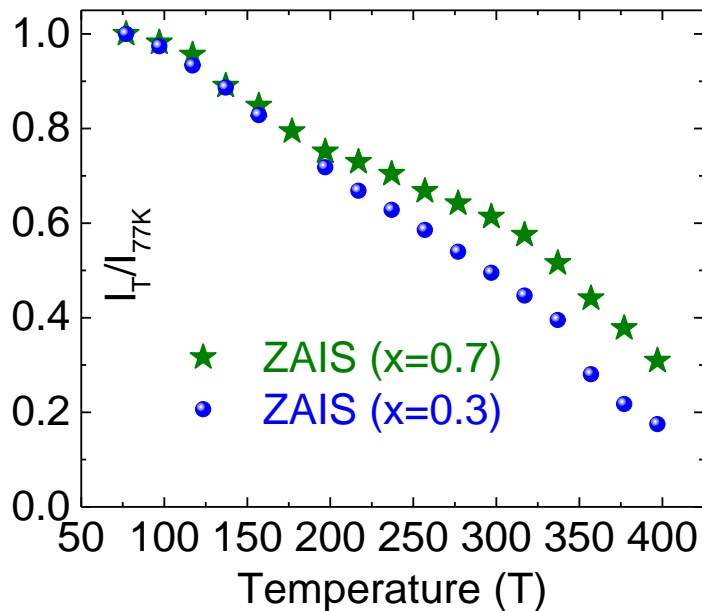


Figure S7 Temperature dependent relative PL intensity change of ZAIS for $x = 0.7$ (green) and $x = 0.3$ (blue) At low temperatures, relative intensity changes are comparable, while at higher temperatures the rate of intensity decay for ZAIS ($x = 0.7$) is slower as compared to ZAIS ($x = 0.3$).

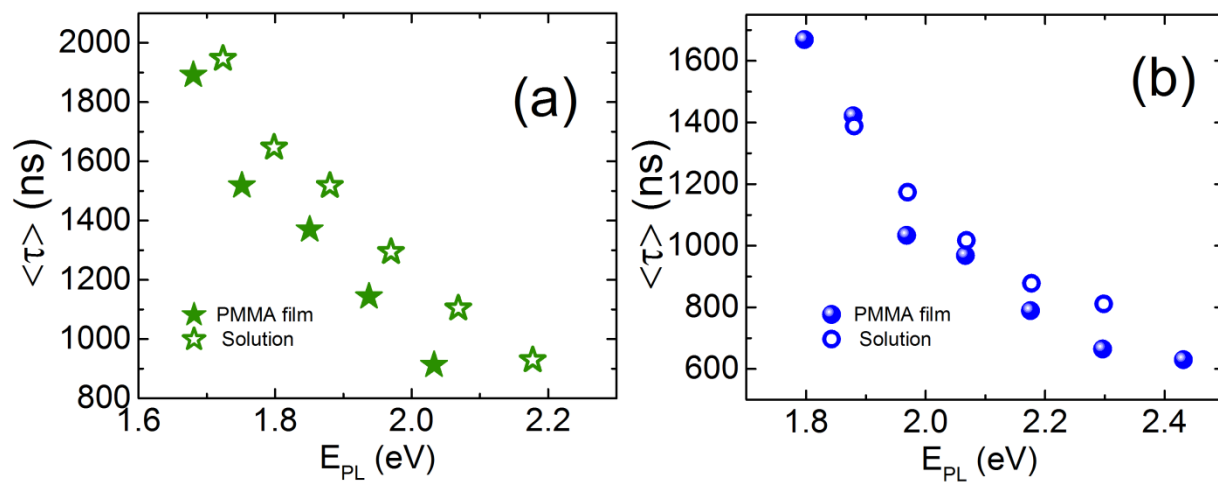


Figure S8 Average lifetimes $\langle \tau \rangle$ of ZAIS of $x=0.7$ (a) and $x=0.3$ (b) monitored at different PL energies in toluene and PMMA film.